Targeting CCL2 with Systemic Delivery of Neutralizing Antibodies Induces Prostate Cancer Tumor Regression *In vivo*

Robert D. Loberg,[1,2] Chi Ying,[2] Matt Craig,[2] Lashon L. Day,[1] Erin Sargent,[1] Chris Neeley,[2] Kirk Wojno,[2] Linda A. Snyder,[4] Li Yan,[3] and Kenneth J. Pienta[1,2]

[1]Department of Urology, University of Michigan Urology Center and [2]Department of Internal Medicine, University of Michigan, Ann Arbor, Michigan; and [3]Department of Hematology/Oncology and [4]Oncology Research, Centocor, Inc., Malvern, Pennsylvania

Abstract

The identification of novel tumor-interactive chemokines and the associated insights into the molecular and cellular basis of tumor-microenvironment interactions have continued to stimulate the development of targeted cancer therapeutics. Recently, we have identified monocyte chemoattractant protein 1 (MCP-1; CCL2) as a prominent regulator of prostate cancer growth and metastasis. Using neutralizing antibodies to human CCL2 (CNTO888) and the mouse homologue CCL2/JE (C1142), we show that treatment with anti-CCL2/JE antibody (2 mg/kg, twice weekly i.p.) attenuated PC-3^{Luc}–mediated overall tumor burden in our *in vivo* model of prostate cancer metastasis by 96% at 5 weeks postintracardiac injection. Anti-CCL2 inhibition was not as effective as docetaxel (40 mg/kg, every week for 3 weeks) as a single agent, but inhibition of CCL2 in combination with docetaxel significantly reduced overall tumor burden compared with docetaxel alone, and induced tumor regression relative to initial tumor burden. These data suggest an interaction between tumor-derived chemokines and host-derived chemokines acting in cooperation to promote tumor cell survival, proliferation, and metastasis. [Cancer Res 2007;67(19):9417–24]

Introduction

Monocyte chemoattractant protein 1 (MCP-1; CCL2) is a member of the CC β chemokine family and is a known chemotactic factor regulating the recruitment of monocytes/macrophages and other inflammatory cells to sites of inflammation via activation of the CCR2 receptor (1). CCL2 was first purified and identified in 1989 from a human glioma (2) and a myelomonocytic cell line (3). The *CCL2* gene maps to chromosome 17q11.2-q12 and comprises a 99-amino-acid precursor protein that when processed and secreted is 75 amino acids in size. CCL2 has been shown to correlate with clinical stage and grade in patients with bladder cancer (4). Recently, several reports have implicated chemokines in the regulation of tumor cell migration resulting in the development and metastasis of several adenocarcinomas, including breast and prostate (5–9). Studies in multiple myeloma have revealed a pivotal role for CCL2 in the "bone homing" phenotype of myeloma cells to the bone marrow compartment (6). Vanderkerken et al. (6) suggested that CCL2 released from the bone marrow endothelial cells stimulates the chemoattraction of 5T multiple myeloma cells as a mechanism of recruitment.

Requests for reprints: Robert D. Loberg, University of Michigan, 7312 CCGC, 1500 East Medical Center Drive, Ann Arbor, MI 48109-0946. Phone: 734-647-3421; Fax: 734-647-9480; E-mail: rloberg@umich.edu.

doi:10.1158/0008-5472.CAN-07-1286

The mechanisms by which CCL2 may promote tumorigenesis and metastasis are currently unknown. CCL2 has been shown previously to promote angiogenesis and promote macrophage recruitment and infiltration in gastric carcinoma (10). The role of macrophages in promoting tumor angiogenesis has been documented and therefore the ability of CCL2 to induce macrophage infiltration may provide a novel mechanism to support neoangiogenic growth of tumors (11–21). In addition to regulating tumor angiogenesis, CCL2 has been shown to induce transendothelial cell migration of myeloma cells, a process that is essential for successful metastasis (22). Initial studies by Mazzucchelli et al. (23) reported that CCL2 is not expressed by prostate cancer cells, but did show strong immunohistochemical evidence of CCL2 expression in the stroma surrounding both benign prostatic hyperplasia and malignant glands. Previously, we and others have shown that prostate cancer cells secrete CCL2 *in vitro* and that this production of CCL2 regulates the migration and proliferation of prostate cancer cell (24). Further, we reported that bone marrow endothelial cells (BMEC) are a significant source of CCL2 and that CCL2 produced by BMECs induces prostate cancer motility/migration (24). Here, we investigate CCL2 as a novel target in prostate cancer growth and metastasis and show that inhibition of tumor-derived CCL2 and host-derived CCL2/JE attenuates tumor growth *in vivo*.

Materials and Methods

Description of CNTO888 and C1142 and control antibodies. CNTO888 is a human IgG1κ antibody that neutralizes human CCL2 (provided by Centocor, Inc.). C1142 is a rat/mouse chimeric antibody that neutralizes mouse CCL2/JE (provided by Centocor). Clinical grade human IgG (huIgG) served as a negative control for CNTO888, whereas C1322 rat/mouse chimeric nonspecific antibody (provided by Centocor) served as a negative control for C1142. CNTO888 does not cross-react with mouse CCL2, and C1142 does not cross-react with human CCL2 (data not shown).

Cell culture. PC-3^{Luc} prostate cancer cell lines were generated as previously described (9) and maintained in RPMI 1640 + 10% fetal bovine serum (FBS; Invitrogen Corp.). Cells were passaged by trypsinization using 1× trypsin + EDTA (Invitrogen), resuspended in appropriate growth medium, and used within 10 passages of each other for consistency.

Proliferation assay. Cells were seeded at a density of 1×10^5/mL for PC-3^{Luc} cells in a 96-well plate in RPMI + 10% FBS. Twenty-four hours after seeding, the medium was changed to either serum-free RPMI supplemented with human recombinant CCL2 (10–100 ng/mL) or RPMI + 10% FBS. Control or neutralizing antibodies (30 μg/mL) were added to the cells 30 min before hrCCL2. Cell growth was determined 72 h later using the WST-1 assay (Pierce Biotech, Inc.) following the manufacturer's instructions. Briefly, WST-1 (Roche) reagent (10 μL/well) was added to each well and incubation continued at 37°C for 2 h. The absorbance at 440 nm was determined using a VersaMax microplate reader (Molecular Devices). Proliferation assays were done in triplicate using six wells per replicate per

condition and reported as a percent of untreated, serum-free medium–only samples.

Migration assay. Human rCCL2 (100 ng/mL) was added to the lower chamber of a 24-well plate in the presence of either control or neutralizing antibodies. Cells were harvested by EDTA release and resuspended in serum-free media at 5×10^4/mL. Cells (2.5×10^4) were added to the upper chamber of the transwell insert and incubated for 24 h at 37°C and 5% CO_2 atmosphere. At the end of the incubation period, the cells were fixed with 4% formaldehyde in PBS for 5 min. Nonadherent cells were removed from inside the inserts with a cotton-tipped applicator. Cells that had migrated to the underside of the insert were stained with 0.5% crystal violet for 5 min and rinsed thoroughly with tap water. Inserts were allowed to dry and the cells were counted using an inverted microscope.

Immunoblot analysis. Cells were lysed in radioimmunoprecipitation assay buffer [50 mmol/L Tris-HCl (pH 7.4), 1% NP40, 150 mmol/L NaCl, 1 mmol/L EDTA, 1 mmol/L phenylmethylsulfonyl fluoride, 1 mmol/L Na_3VO_4, 1 mmol/L NaF, 1 μmol/L okadaic acid and 1 μg/mL aprotinin, leupeptin, and pepstatin]. Proteins were separated under reducing conditions by SDS-PAGE and transferred onto nitrocellulose membrane. The membranes were blocked with 5% milk in TBST (0.1% Tween in TBS) for 1 h at room temperature followed by incubation overnight at 4°C with phosphorylated Akt, total Akt, phosphorylated p70S6 kinase, total p70S6 kinase, phosphorylated p44/p42, and total p44/p42 primary antibodies (Cell Signaling, Inc.). Membranes were washed thrice before incubation with horseradish peroxidase–conjugated secondary antibodies (Cell Signaling) for 1 h at room temperature. Protein expression was visualized by enhanced chemiluminescence (Promega) and quantitated using Image J software (National Cancer Institute).

Tissue microarray analysis. Tissue microarray (TMA) were manufactured as previously described (2). Tissue from 84 patients (normal, 10; benign prostatic hyperplasia, 8; prostatic interepithelial neoplasia, 9; prostate cancer, 48) were retrieved from needle core biopsies and placed in paraffin blocks. Tissue cores of 0.6 mm in diameter were arrayed vertically in triplicate in a new paraffin block (a total of 252 cores were analyzed). For the metastasis array, 133 metastatic lesions (bone, 19; soft tissue, 96) were retrieved from the Rapid Autopsy Program at the University of Michigan and analyzed in triplicate (399 total cores analyzed). Array slides were stained with immunoperoxidase stains using anti-CCR2 (Abcam, Inc.) and the DAKO AutoStainer and EnVision + Peroxidase development kits from DAKO Cytomation. Microwave antigen retrieval was done in a citrate buffer (pH 6.0) for 10 min on all slides. Arrays were analyzed by a blinded pathologist and percentage and intensity of epithelial cells stained were recorded. Staining intensity was ranked on a scale from 0 to 3 (0, negative; 1, weak; 2, moderate; 3, strong intensity staining). Data are presented as mean ± SE.

***In vivo* bioluminescent model of prostate cancer growth.** Bioluminescent imaging of PC-3^{Luc} was done as previously described through The University of Michigan Small Animal Imaging Resource facility (24). Briefly, PC-3^{Luc} cells were introduced into male severe combined immunodeficient (SCID) mice (5–6 weeks of age) by intracardiac injections. Mice were serially imaged weekly for up to 12 weeks using a CCD IVIS system with a 50-mm lens (Xenogen Corp.) and the results were analyzed using LivingImage software (Xenogen). Mice were allotted into groups and treatment began at week 2 postintracardiac injection. Mice (n = 140) were ranked in numerical order based on their week 1 photons per second value and animals were allotted (assigned) to groups sequentially by placing them into groups 1 through 14 beginning with the highest photons per second value and repeating allotment until all animals were placed in a group (final groups n = 10). Animals were allotted rather than randomly divided to prevent skewed data due to randomization. Mice received 2 mg/kg antibody twice weekly by i.p. injection (for up to 8 weeks) and/or 40 mg/kg docetaxel by i.p. injection once per week for 3 weeks. Mice were injected with luciferin (40 mg/mL) i.p. and ventral images were acquired 15 min postinjection under 1.75% isofluorane/air anesthesia. Total tumor burden of each animal was calculated using regions of interest (ROI) that encompassed the entire animal. For tibia-specific measurements, ROI values were recorded for each individual tibia. The number of tibia-specific lesions was quantified by visual assessment of a luminescent signal evident at week 5 and the total number of lesions per animal was recorded (0, 1, or 2 lesions per animal).

Statistics. Data was analyzed with GraphPad Prism software. A one-way ANOVA analysis was used with Bonferroni's post hoc analysis for comparison between multiple groups. A Student's t test was used for comparison between two groups. Significance was defined as a P value of <0.05. For analyses of the *in vivo* tumor burden data for the groups receiving docetaxel in combination with antibodies, a repeated measures model was fit to the data assuming a first-order autocorrelation covariance structure. Natural splines were used to flexibly model the curvature of trends by the time profiles. A logarithmic scale was used to better satisfy underlying statistical model assumptions of variability and normal distribution shape. Pairwise comparisons among the groups were made at each of the time points. P values of ≤0.05 were deemed significant unless noted otherwise.

Results

CNTO888 inhibited PC-3^{Luc} cell proliferation and migration *in vitro*. To determine the potential of inhibiting CCL2 and the role CCL2 inhibition would play on prostate cancer cells, PC-3 cells were stimulated *in vitro* with hrCCL2 (10–100 ng/mL) for 72 h in the presence of an anti-human CCL2 neutralizing antibody (CNTO888; 30 μg/mL) or/and anti-mouse CCL2/JE neutralizing antibody (C1142; 30 μg/mL; Fig. 1*A*). An increase in cell viability, as a measure of proliferation, was determined using the WST-1 method. The data revealed an inhibition of hrCCL2-induced proliferation by CNTO888 compared with the human IgG control antibody and the anti-CCL2/JE (C1142) antibody [CCL2 (10 ng/mL): 136.2 ± 7.81%; CNTO888: 112.52 ± 10.2%; C1142: 132.18 ± 3.48%; CNTO888 + C1142: 108.22 ± 9.89%, mean ± SD] and [CCL2 (100 ng/mL): 168.15 ± 5.44%; CNTO888: 132.93 ± 17.08%; C1142: 165.92 ± 15.22%; CNTO888 + C1142: 118.93 ± 19.29%, mean ± SD]. Similarly, CNTO888 attenuated hrCCL2-induced migration compared with either control or C1142 antibodies [control: 393 ± 67; CNTO888: 217 ± 29; C1142: 371 ± 36; CNTO888 + C1142: 209 ± 24, mean ± SD; Fig. 1*B*]. Previously, we reported an up-regulation of Akt activity in PC-3 cells stimulated with hrCCL2 (9). The presence of CNTO888 attenuated Akt, p70S6 kinase, and p44/p42 mitogen-activated protein kinase activation in response to hrCCL2 stimulation (Fig. 1*C*). These results indicated that prostate cancer cells responded to CCL2 by enhanced proliferation and migration, and that an anti-CCL2 antibody could inhibit these activities.

CCR2 expression correlates with prostate cancer progression and metastasis. To determine the clinical importance of targeting the CCL2/CCR2 signaling pathway in prostate cancer, CCR2 receptor expression on prostate epithelial cells was analyzed by TMA in collaboration with the TMA core at the University of Michigan (Fig. 2). Prostate cancer epithelial cell CCR2 expression showed a correlation with proliferative inflammatory atrophy and Gleason score with significantly elevated levels of expression in Gleason >7 tumors (Fig. 2*H*). TMA analysis revealed a significant increase in CCR2 expression in metastatic tissue compared with primary prostate cancer, although no significant difference in CCR2 expression was observed when soft tissue metastases were compared with bone metastases (Fig. 2*G* and *I*).

Anti-CCL2 antibodies decrease tumor burden *in vivo*. To visualize the effects of CCL2 inhibition on prostate cancer, we used an *in vivo* model of prostate cancer growth as previously described (9). PC-3^{Luc} cells were introduced into male SCID mice (n = 8 per treatment group) by intracardiac injection and tumor growth was monitored weekly. At week 1 postinjection, 100% of mice showed at least one focal point of photon emission. Serial bioluminescent

images were taken weekly for 5 weeks. Beginning on day 14, animals were allotted into five treatment groups based on their individual day 5 bioluminescent image. Treatment groups received the following treatment/antibodies: (*a*) PBS control, (*b*) huIgG control, (*c*) anti-human CCL2 CNTO888, (*d*) mouse control antibody (C1322), and (*e*) anti-mouse CCL2/JE (C1142). Antibodies were given at 2 mg/kg twice weekly i.p. for 3 weeks. At day 35, total tumor burden per animal was quantified and efficacy between treatment groups was ascertained (Fig. 3*A*). No significant toxicity was observed in any treatment group and mean body weights were not significantly different with antibody therapy (Fig. 3*B*). Administration of anti-human CCL2 antibody (CNTO888) reduced overall tumor burden by 47% compared with the PBS control group; however, significance was not achieved (Fig. 3*C–E*). Additionally, administration of an anti-mouse CCL2/JE antibody (C1142) significantly reduced overall tumor burden by 96% compared with the PBS control group ($P < 0.001$) and compared with the mouse control antibody group ($P < 0.05$; Fig. 3*C, F,* and *G*). There was no significant difference between the PBS control and the huIgG or the mouse control antibodies.

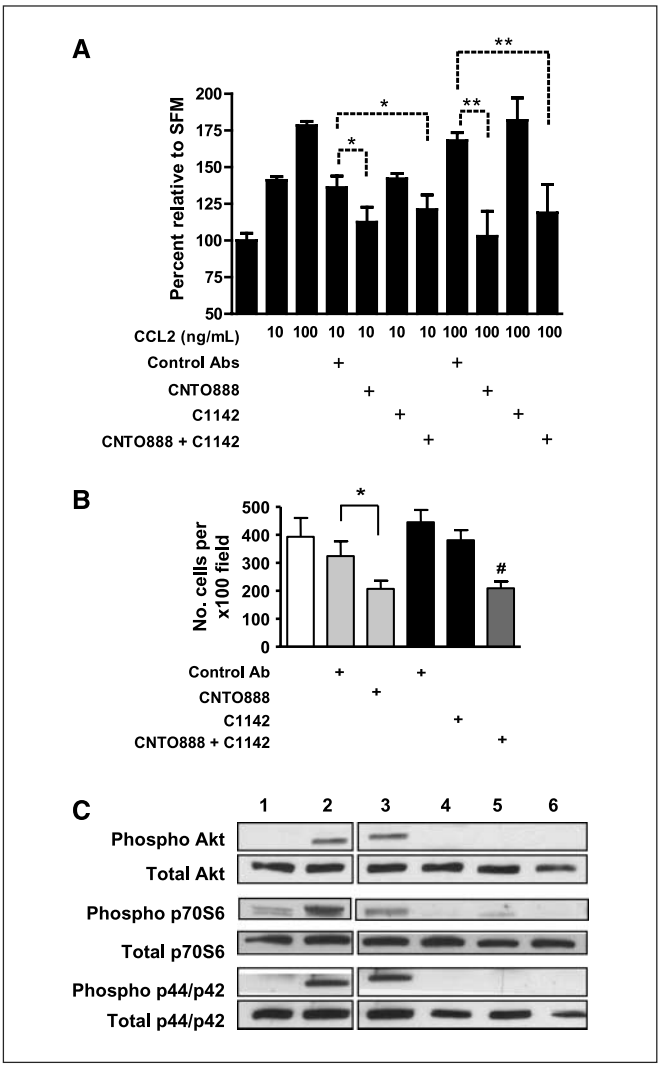

Figure 1. CNTO888 inhibits PC-3^{Luc} cell proliferation and migration *in vitro*. *A,* PC-3^{Luc} cells were stimulated with CCL2 (10 or 100 ng/mL) for 72 h in the presence or absence of CNTO888 (30 μg/mL), C1142 (30 μg/mL), or CNTO888 + C1142 (30 μg/mL each). The control antibody (*Ab*) for CNTO888 is anti-huIgG and the control antibody for C1142 is C1322 (a rat/mouse chimeric nonspecific antibody). Cell viability was measured by WST-1. *Columns,* mean percentage of serum-free medium control; *bars,* SD (*, $P < 0.05$; **, $P < 0.01$). *SFM,* serum-free medium. *B,* PC-3^{Luc} cell migration was measured in response to hrCCL2 (100 ng/mL). The number of cells migrating per ×100 objective field was manually counted by microscopy. *Columns,* mean (*, $P < 0.01$; #, $P < 0.01$ compared with control); *bars,* SD. *C,* immunoblot analysis of Akt, p70S6 kinase, and mitogen-activated protein kinase p44/p42 activation. Representative immunoblots from four independent experiments. *1,* control; *2,* CCL2 (100 ng/mL, 24 h); *3,* CCL2 (100 ng/mL) + C1142 (30 μg/mL); *4,* CCL2 (100 ng/mL) + CNTO888 (30 μg/mL); *5,* C1142 (30 μg/mL); *6,* CNTO888 (30 μg/mL).

Comparison of tumor burden between treatment groups in a specific bone site (the tibia) revealed similar significant inhibition of tumor growth (Fig. 4). As prostate cancer metastases present predominantly as bone lesions, and as the tibia is a common site of metastasis for PC-3^{Luc} cells as described previously (25), we analyzed tumor burden localized in the tibias of the intracardiac-injected mice described above. Tibia-specific tumor burden was analyzed for 5 weeks postintracardiac injection (Fig. 4*A*). Tumor burden on day 35 was used to compare efficacy of treatment between treatment groups as stated above. Administration of anti-human CCL2 antibody CNTO888 significantly reduced tibia-specific tumor burden by 87% compared with the PBS control group ($P < 0.001$; Fig. 4*B*) and compared with the huIgG control antibody ($P < 0.01$; Fig. 4*B*). Additionally, administration of an anti-mouse CCL2/JE antibody (C1142) significantly reduced tibia-specific tumor burden by 95% compared with the PBS control group ($P < 0.001$; Fig. 4*B*) and compared with the C1322 mouse control antibody ($P < 0.001$; Fig. 4*B*). Further, administration of the anti-mouse CCL2/JE (C1142) significantly reduced the number of total bone-specific metastatic lesions as identified by visual confirmation of luciferase signal upon imaging ($P < 0.05$; Fig. 4*C*). These results indicate that inhibition of either the host stromal-derived mouse CCL2 or the tumor-derived human CCL2 can attenuate the formation of bone metastases, suggesting that each may play a role in this process.

Single-agent anti-CCL2 compared with single-agent docetaxel *in vivo*. To further determine the efficacy of CCL2 inhibition in advanced prostate cancer, CNTO888 and C1142 as single agents were compared with single-agent docetaxel at a maximally tolerated dose (MTD) that we had previously established (Fig. 5*A*). CNTO888 (2 mg/kg, i.p. twice weekly) showed a trend toward reduction in tumor burden by day 35 (23% decrease compared with PBS-treated animals) whereas C1142 (2 mg/kg, i.p. twice weekly) and C1142 + CNTO888 (2 mg/kg each, i.p. twice weekly) resulted in a significant decrease in total tumor burden (73% and 71% decrease compared with PBS-treated animals, respectively). However, neither C1142 nor CNTO888 + C1142 was as effective as a single agent when compared with single-agent docetaxel (40 mg/kg, i.p., every week for 3 weeks; 96% decrease compared with PBS-treated animals at day 35; Fig. 5*B*). The results from this second study support the initial *in vivo* study demonstrating that inhibition of host-derived CCL2 (C1142) significantly attenuated tumor burden in mice (Fig. 3*A* and *B*).

Anti-CCL2 antibodies in combination with docetaxel induce tumor regression *in vivo*. We hypothesized that the role of CCL2 in the tumor microenvironment was to support tumor establishment and promote growth. Currently, docetaxel is the only chemotherapy that has shown a survival benefit for patients with hormone-refractory prostate cancer; however, only 45% of patients respond to this chemotherapy (26). Thus, to determine the efficacy of combination therapy with docetaxel and CCL2 inhibition in advanced

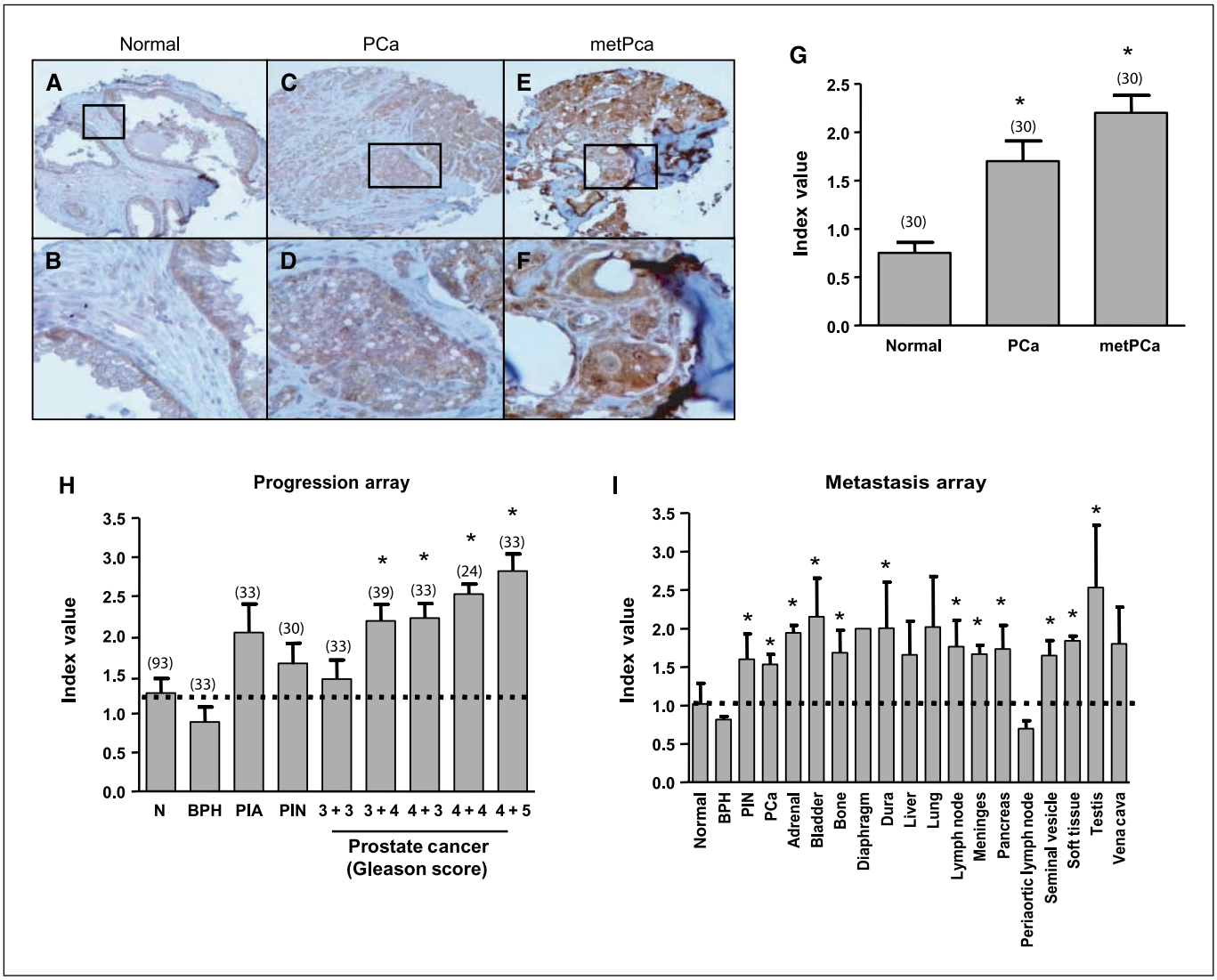

Figure 2. CCR2 expression correlates with prostate cancer progression and metastasis. CCR2 expression was analyzed by tissue microarray analysis and showed epithelial cell staining in normal (*A* and *B*), primary prostate cancer (*PCa*; *C* and *D*), and metastatic prostate cancer (*metPca*; *E* and *F*). *, $P < 0.05$ compared with normal (*N*). Graphical analysis of TMAs showed a significant increase in CCR2 expression (*G*) and correlated with disease progression and Gleason score (*H*). No difference was seen in CCR2 expression between soft tissue metastases and bone metastases (*I*). *, $P < 0.05$ compared with normal. *BPH,* benign prostatic hyperplasia; *PIN,* prostatic interepithelial neoplasia.

prostate cancer, CNTO888 and C1142 in combination with docetaxel were compared with single-agent docetaxel (Fig. 6*A*). Treatment was initiated on week 2 postintracardiac injection, and mice received either single-agent docetaxel (MTD 40 mg/kg, i.p., every week for 3 weeks) or docetaxel in combination with anti-CCL2 antibodies (2 mg/kg, i.p. twice weekly). Docetaxel treatment was stopped after 3 weeks and animals were maintained on antibodies for an additional 3 weeks (until week 8) after which all treatment was stopped and tumor burden was monitored. Mice treated with docetaxel alone displayed a decrease in tumor burden while receiving therapy; however, once the treatment stopped, the mice began to develop additional tumor burden. Mice treated with a combination of docetaxel and anti-CCL2 antibodies showed a significant reduction of tumor burden compared with animals receiving single-agent docetaxel ($P < 0.0001$; Fig. 6*A*). Furthermore, continued administration of anti-CCL2 antibodies after treatment with docetaxel was discontinued showed that the mice maintained the decreased tumor burden compared with mice that did not receive antibody therapy (percent tumor burden at week 6 compared with week 2: docetaxel 39.7%, docetaxel + CNTO888 121.03%, docetaxel + C1142 80.28%, docetaxel + CNTO888/C1142 58.91%) and (percent tumor burden at week 9 compared with week 2: docetaxel 208.72%, docetaxel + CNTO888 66.68%, docetaxel + C1142 26.22%, docetaxel + CNTO888/C1142 25.89%; Fig. 6*B*). Once antibody treatment was discontinued, tumor burden began to increase again until the mice were euthanized at week 12, suggesting that the antibody treatment had controlled tumor growth. The docetaxel groups were then analyzed statistically for evidence of tumor regression. The group treated with docetaxel alone showed a statistically significant increase in tumor burden, relative to week 2, from week 5 to the end of the study. No statistically significant changes relative to week 2 were observed in the docetaxel

+ CNTO888 group. In contrast, statistically significant decreases in tumor burden relative to week 2 were found for weeks 6 through 9 in the docetaxel + C1142 group ($P \leq 0.039$). The most dramatic results were seen in the docetaxel + CNTO888/C1142 group, in which significant regression was evident at week 4 ($P = 0.031$), continued through week 9 ($P \leq 0.001$), with tumor regrowth evident from week 10 to study termination. These results show that the combination of docetaxel and anti-CCL2 antibodies was more efficacious than docetaxel alone by inducing tumor regression, and that the antibody therapy played a role in the maintenance of tumor regression.

Discussion

Tumor progression is regulated by various intrinsic and extrinsic (microenvironment) factors. It is now well accepted that cancer cells exist in a complex environment in which they interact with a wide variety of stromal cells, including the multiple cell types that make up the immune system of the host. Many of these interactions are mediated by chemokines. The roles of chemokines in tumorigenesis have been shown to be diverse, but include both negative and positive regulation of inflammatory cells, chemoattraction of tumor cells to metastatic sites, regulation of angiogenesis, and direct regulation of proliferation of cancer cells (27). One of the initial descriptions of CCL2 was as a "tumor-derived chemotactic factor" and it is found at high levels in multiple tumor types (28, 29). It has been shown to be a potent chemoattractant for several cell types of the immune system, including monocytes, natural killer cells, memory T cells, and immature dendritic cells, thereby mediating multiple proinflammatory effects, including neoangiogenesis (28–34). In addition, CCL2 has been shown to have direct effects on tumor cells in an autocrine and paracrine fashion in multiple cancers, including breast, lung, cervix, ovary, sarcoma, and prostate (24, 28, 35–37).

Our *in vivo* data reported here confirm these reports and support an important role for CCL2 in prostate cancer tumorigenesis and metastasis. The availability of both human-specific and mouse-specific antibodies has allowed us to dissect the relative importance of tumor-derived and host-derived CCL2 pathways on tumorigenesis. Our experiments show that targeting the CCL2 contributed by the human cancer cells modestly inhibits tumor growth and suggests that CCL2 secreted by the tumor cells contributes to the CCL2-dependent tumor growth via a paracrine/autocrine mechanism. However, antitumor efficacy derived from targeting the mouse CCL2 suggests that host-derived CCL2,

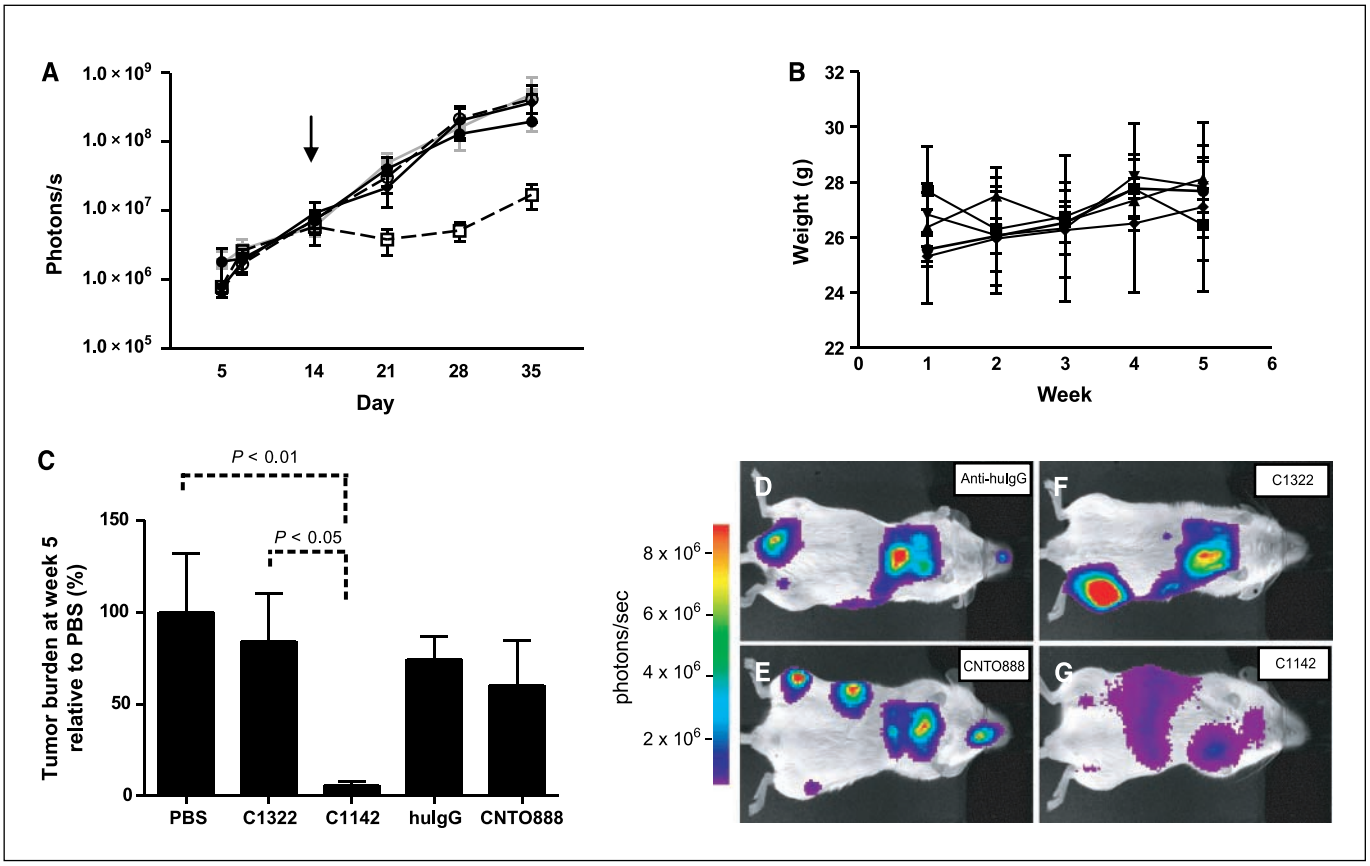

Figure 3. *In vivo* bioluminescent imaging of PC-3^{Luc} cell metastasis during systemic CCL2-targeted therapy. *A,* mice (n = 8 mice per group) received PC-3^{Luc} cells by intracardiac injection. Beginning on day 14, mice received PBS (▫), huIgG control antibody (♦), mouse antibody control C1322 (○), anti-human CCL2 CNTO888 (●), or anti-CCL2/JE C1142 (□) at 2 mg/kg twice weekly by i.p. injection (*arrow,* when treatment began). Overall tumor burden was monitored weekly and recorded as photons per second. *Solid lines*, human antibodies; *dashed lines*, mouse antibodies. *B,* mean body weights were recorded and displayed for each group [*PBS* (■), huIgG control antibody (▲), mouse antibody control C1322 (▼), antihuman CCL2 CNT0888 (♦), or anti-CCL2/JE *C*1142 (●)]. No significant change in body weight was observed between treatment groups. *C,* at day 35, overall tumor burden was compared between groups and percentage reduction of overall tumor burden was reported ($P < 0.01$, C1142 compared with PBS). *D* to *G,* representative pictures illustrate images captured on day 35 from representative animals from each group: *D,* huIgG; *E,* CNTO888; *F,* C1322; and *G,* C1142.

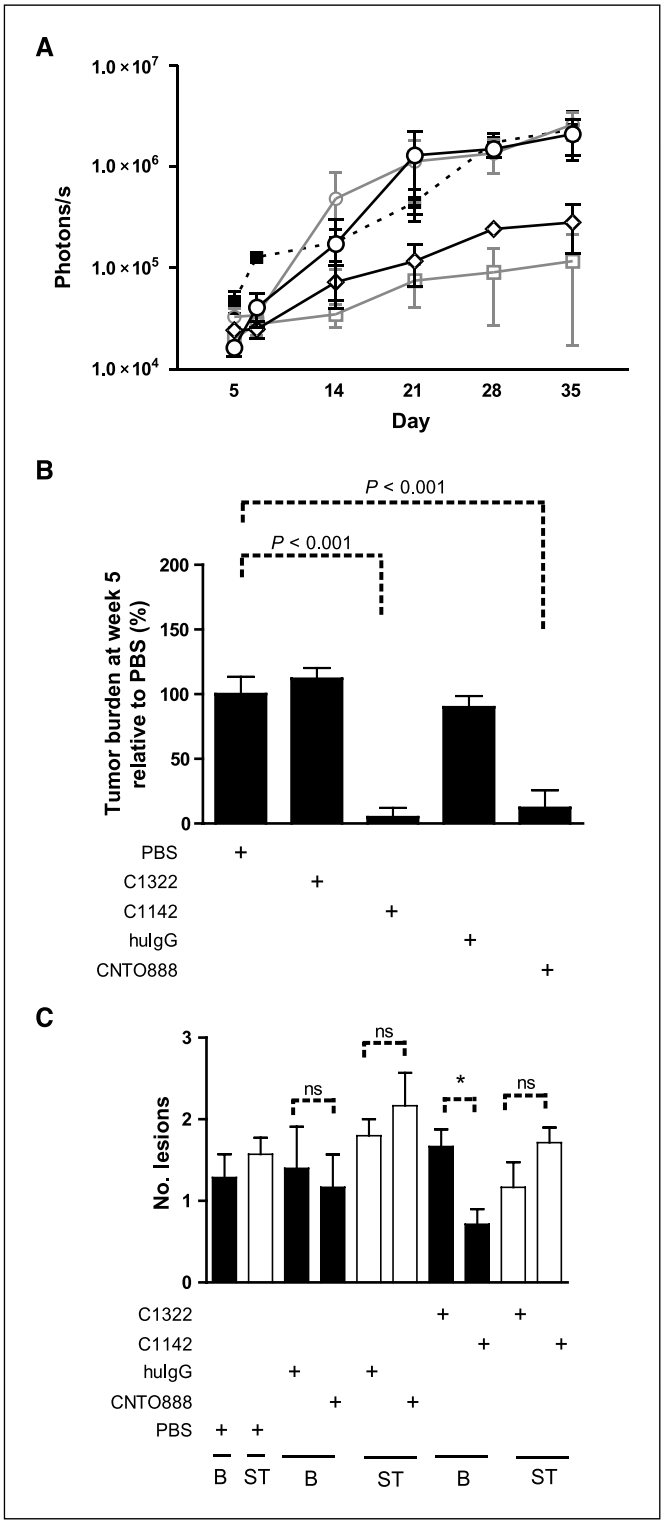

Figure 4. Anti-CCL2 antibodies decrease bone-specific tumor burden *in vivo* (n = 8 per group). *A,* tumor burden in the tibia was analyzed independently and tibia-specific tumor burden was assessed over the 5-wks treatment period. PBS (■), huIgG control antibody (○) mouse antibody control C1322 (○), antihuman CCL2 CNT0888 (◇), or anti-CCL2/JE C1142 (□). *B,* final day (day 35) tibia-specific tumor burden showed significant reduction by CCL2 inhibition, by either antitumor or antihost CCL2 antibodies compared with PBS control group ($P < 0.001$). *C,* the number of metastases was identified by gross examination of luciferase signal for each animal and graphed as the total number of soft tissue (*ST, white columns*) versus bone (*B, black columns*) metastases (*, $P < 0.05$; ns, not significant).

possibly from the bone marrow endothelium, plays a prominent role in regulating prostate cancer growth and metastasis and may contribute to the bone metastatic phenotype characteristic of prostate cancer (24). The data suggest that there is a cooperation between tumor cell–derived CCL2 and host-derived CCL2 in promoting tumor growth, and that the host-derived CCL2 may contribute specifically to the ability of prostate cancer to metastasize and successfully colonize distant sites. One potential mechanism by which host-derived CCL2 confers a significant growth advantage to prostate cancer cells in the bone microenvironment is by the regulation of osteoclast differentiation and activation. CCL2 has been shown to be important in osteoclast

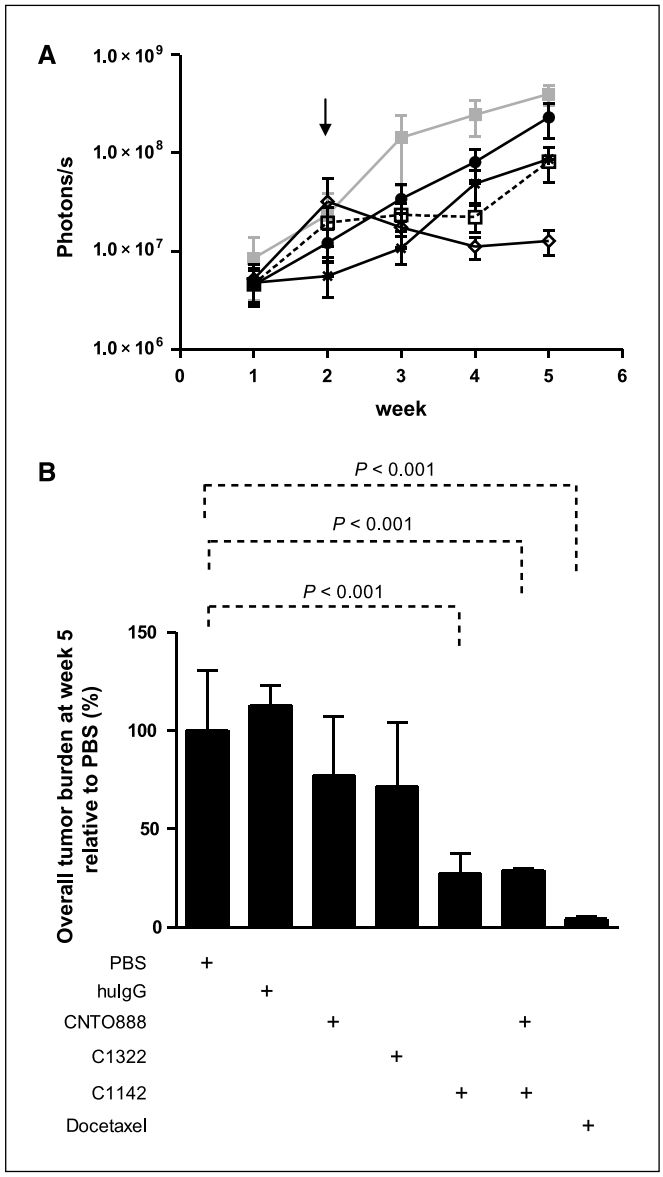

Figure 5. Efficacy of single-agent anti-CCL2 antibodies compared with single-agent docetaxel *in vivo. A,* inhibition of CCL2 was compared with docetaxel (MTD 40 mg/kg) by bioluminescent imaging and quantification of total tumor burden. Mice received PC-3^{Luc} cells by intracardiac injection (n = 10 per group). Beginning on day 14, mice received PBS (▣), (CNTO888 (●), C1142), CNTO888 + C1142 (✱), or docetaxel (◇) by i.p. injection (*arrow,* when treatment began). *Solid lines*, human antibodies; *dashed lines*, mouse antibodies. *B,* total tumor burden at day 35 was compared between groups and percent reduction of overall tumor burden was reported ($P < 0.001$ compared with PBS control group).

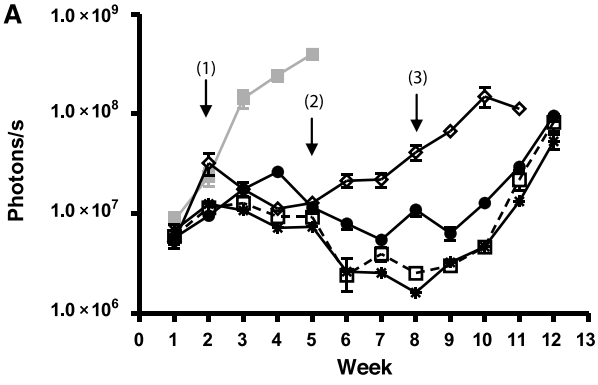

B

No. animals per group	Treatment	week 6		week 9		week 12	
		#No.	%	#No.	%	#No.	%
10	PBS	1 of 10	1,273.4				
10	huIgG	2 of 10	1,578.3				
9	C1322	0 of 9	2,574.5				
9	CNTO888	1 of 9	1,898.0				
9	C1142	0 of 9	419.8				
9	CNTO888 + C1142	0 of 9	1,552.6				
9	Taxotere	2 of 9	***39.6*** **	1 of 9	208.72		
9	Taxotere + CNTO888	6 of 9	121.0	3 of 9	***66.7*** **	2 of 9	1,009.2
9	Taxotere + C1142	7 of 9	***80.2*** **	4 of 9	***26.2*** **	3 of 9	719.1
9	Taxotere + CNTO888 + C1142	9 of 9	***58.9*** **	6 of 9	***25.9*** **	3 of 9	423.0

week 6 = First week after cessation of Taxotere
week 9 = First week after cessation of Antibodies

Figure 6. Anti-CCL2 antibodies in combination with docetaxel induce tumor regression *in vivo. A,* inhibition of CCL2 in combination with docetaxel (MTD 40 mg/kg) was assessed by bioluminescent imaging and quantification of total tumor burden and compared with docetaxel alone. Mice received PC-3^{Luc} cells by intracardiac injection. Beginning on day 14, mice received PBS (▫), docetaxel + CNTO888 (●), docetaxel + C1142 (□), docetaxel + CNTO888 + C1142 (✱), or docetaxel (◇) by i.p. injection. Docetaxel was administered every week for 3 wks (weeks 2–4), whereas antibodies were delivered twice per week for 6 wks (weeks 2–8). On week 8, all antibody treatments were stopped and tumor progression was monitored to week 12. [*arrow (1),* initiation of treatment; *arrow (2),* cessation of docetaxel; *arrow (3),* cessation of antibody therapy]. Statistical significance was determined at week 10 between the docetaxel group and the combination docetaxel + antibody groups. Overall significance by ANOVA revealed a significant difference between docetaxel only and docetaxel + antibody groups ($P < 0.0001$). Individual *t* tests revealed significant differences between docetaxel only and docetaxel + CNTO888 ($P = 0.0003$), docetaxel + C1142 ($P = 0.0001$), or docetaxel + C1142 + CNTO888 ($P = 0.0001$). *Solid lines*, human antibodies; *dashed lines*, mouse antibodies. *B,* combination docetaxel and anti-CCL2 antibodies induced tumor regression compared with docetaxel or antibodies alone at weeks 6 to 9. The number of animals that showed tumor regression (*#No.*) and the mean percentage reduction in total tumor burden for each group compared with their respective week 2 measurements are shown with the groups demonstrating a decrease in tumor burden identified (**).

activation in combination with RANKL (38). Up-regulation of CCL2 in the bone microenvironment by the presence of primary prostate cancer may induce a precipitating event of ostecolysis, resulting in increased prostate cancer cell seeding and growth in the bone marrow compartment. In addition to regulating osteolysis, CCL2 is known to promote infiltration of immune cells into neoplastic tissue and monocytes have been shown to secrete high levels of CCL2 in response to inflammation and injury (39). In our current model using SCID mice (T cell and B cell deficient), this effect is most likely through recruitment of host monocytes/macrophages. In addition, mice produce a homologue of CCL2, CCL12 (also known as MCP-5, not expressed in humans), which has been shown to bind and activate the human and mouse CCR2 receptor (40). The studies presented here support a role of CCL2 in prostate cancer growth but the significance of CCL2 blockade may be underestimated by the influence of additional chemokines that can activate the CCR2 receptor on prostate cancer cells. In spite of promiscuity among the chemokines and chemokine receptors, it is clear that CCL2 plays an important role in the development and progression of prostate cancer by directly stimulating prostate cancer epithelial cells and by regulating monocyte/macrophage infiltration into prostate tumors. Previous studies have shown that CCL2 is an important chemokine that regulates infiltration of tumor-associated macrophages (TAM) into neoplastic tissue (28); further experiments are required to determine the role of TAMs on prostate cancer metastasis and the role CCL2 plays in regulating TAM infiltration.

The data presented here suggest that anti-CCL2 therapy alone is not sufficient to eradicate established disease. Our data indicate that administration of an anti-CCL2 antibody alone or in combination with docetaxel may represent an important therapeutic strategy for the treatment of prostate cancer by debulking established disease with chemotherapeutics. Single-agent treatment reduced tumor burden in animals, with a much greater effect observed with the use of the anti-mouse CCL2. These results suggest that the role of the host stromal-derived CCL2 play a more prominent role in prostate cancer growth and metastasis than that of the tumor-derived CCL2 in the context of this androgen-independent prostate tumor model. Given that CCL2 also regulates Th2 T cells and that CCL2 knockout mice show impaired Th2 immunity but intact Th1 immune responses (41), the effect of CCL2 inhibition may even be greater in immunocompetent hosts (humans). Furthermore, the addition of docetaxel to antibody treatment induced tumor regression *in vivo*, which was significantly greater than that observed with either the antibody treatments or docetaxel alone (Fig. 6*B*). Intriguingly, continuing animals on antibody therapy after the cessation of docetaxel maintained tumor regression and the development of

additional tumor burden compared with animals receiving docetaxel alone. Further statistical analysis showed that the fold change in tumor burden compared with week 2 (the measurement before initiation of treatments) showed statistically significant decreases for weeks 6 through 9 in the docetaxel + C1142 group. Additionally, statistically significant decreases in tumor burden compared with week 2 were observed for weeks 4 through 10 in the docetaxel + CNTO888/C1142 group. Docetaxel alone showed statistically significant increases from week 5 to the end of the study. The statistical analyses further support the role of host-derived CCL2 as more prominent in the establishment and maintenance of prostate cancer and showed that antibodies combined with docetaxel induced a significant tumor regression compared with docetaxel alone.

In summary, we have hypothesized and shown that CCL2 secreted from the tumor cell acts in a paracrine/autocrine fashion to promote cell survival and growth, whereas CCL2 secreted from the host environment, specifically the bone marrow endothelial cells, stimulates migration and proliferation in the bone microenvironment (24). We present data here that implicate CCL2 in prostate cancer pathogenesis and identifies CCL2 as a potential novel therapeutic target. Further work is required to delineate the role of tumor-derived CCL2 and host-derived CCL2 in prostate cancer tumorigenesis and metastasis.

Acknowledgments

Received 4/9/2007; revised 6/28/2007; accepted 7/18/2007.

Grant support: NIH grant PO1 CA093900-01 (R.D. Loberg and K.J. Pienta) and University of Michigan Prostate Specialized Programs of Research Excellence Career Development Award P50 CA69568-06A (R.D. Loberg). Dr. Pienta is an American Cancer Society Clinical Research Professor.

The costs of publication of this article were defrayed in part by the payment of page charges. This article must therefore be hereby marked *advertisement* in accordance with 18 U.S.C. Section 1734 solely to indicate this fact.

We thank Dr. Bill Pikounis for conducting the statistical analysis of the docetaxel study and Karen Giles for manuscript preparation.

References

1. Charo IF, Taubman MB. Chemokines in the pathogenesis of vascular disease. Circ Res 2004;95:858–66.
2. Yoshimura T, Robinson EA, Tanaka S, Appella E, Leonard EJ. Purification and amino acid analysis of two human monocyte chemoattractants produced by phytohemagglutinin-stimulated human blood mononuclear leukocytes. J Immunol 1989;142:1956–62.
3. Matsushima K, Oppenheim JJ. Interleukin 8 and MCAF: novel inflammatory cytokines inducible by IL 1 and TNF. Cytokine 1989;1:2–13.
4. Amann B, Perabo FG, Wirger A, Hugenschmidt H, Schultze-Seemann W. Urinary levels of monocyte chemo-attractant protein-1 correlate with tumour stage and grade in patients with bladder cancer. Br J Urol 1998;82:118–21.
5. Youngs SJ, Ali SA, Taub DD, Rees RC. Chemokines induce migrational responses in human breast carcinoma cell lines. Int J Cancer 1997;71:257–66.
6. Vanderkerken K, Vande Broek I, Eizirik DL, et al. Monocyte chemoattractant protein-1 (CCL2), secreted by bone marrow endothelial cells, induces chemoattraction of 5T multiple myeloma cells. Clin Exp Metastasis 2002;19:87–90.
7. Sun YX, Wang J, Shelburne CE, et al. Expression of CXCR4 and CXCL12 (SDF-1) in human prostate cancers (PCa) *in vivo*. J Cell Biochem 2003;89:462–73.
8. Nouh MA, Eissa SA, Zaki SA, El-Maghraby SM, Kadry DY. Importance of serum IL-18 and RANTES as markers for breast carcinoma progression. J Egypt Natl Canc Inst 2005;17:51–5.
9. Loberg RD, Day LL, Dunn R, Kalikin LM, Pienta KJ. Inhibition of decay accelerating factor (CD55) attenuates prostate cancer growth and survival *in vivo*. Neoplasia 2006;8:69–78.
10. Kuroda T, Kitadai Y, Tanaka S, et al. Monocyte chemoattractant protein-1 transfection induces angiogenesis and tumorigenesis of gastric carcinoma in nude mice via macrophage recruitment. Clin Cancer Res 2005; 11:7629–36.
11. Molema G, Meijer DK, de Leij LF. Tumor vasculature targeted therapies: getting the players organized. Biochem Pharmacol 1998;55:1939–45.
12. Connolly JM, Rose DP. Angiogenesis in two human prostate cancer cell lines with differing metastatic potential when growing as solid tumors in nude mice. J Urol 1998;160:932–6.
13. Oliner J, Min H, Leal J, et al. Suppression of angiogenesis and tumor growth by selective inhibition of angiopoietin-2. Cancer Cell 2004;6:507–16.
14. Kim KJ, Li B, Winer J, et al. Inhibition of vascular endothelial growth factor-induced angiogenesis suppresses tumour growth *in vivo*. Nature 1993;362:841–4.
15. Millauer B, Shawver LK, Plate KH, Risau W, Ullrich A. Glioblastoma growth inhibited *in vivo* by a dominant-negative Flk-1 mutant. Nature 1994;367:576–9.
16. Ikeda Y, Hayashi I, Kamoshita E, et al. Host stromal bradykinin B2 receptor signaling facilitates tumor-associated angiogenesis and tumor growth. Cancer Res 2004;64:5178–85.
17. Kumar H, Heer K, Lee PW, et al. Preoperative serum vascular endothelial growth factor can predict stage in colorectal cancer. Clin Cancer Res 1998;4:1279–85.
18. Maeda K, Chung YS, Ogawa Y, et al. Prognostic value of vascular endothelial growth factor expression in gastric carcinoma. Cancer 1996;77:858–63.
19. Toi M, Inada K, Suzuki H, Tominaga T. Tumor angiogenesis in breast cancer: its importance as a prognostic indicator and the association with vascular endothelial growth factor expression. Breast Cancer Res Treat 1995;36:193–204.
20. Korfee S, Gauler T, Hepp R, Pottgen C, Eberhardt W. New targeted treatments in lung cancer—overview of clinical trials. Lung Cancer 2004;45:S199–208.
21. Hicklin DJ, Ellis LM. Role of the vascular endothelial growth factor pathway in tumor growth and angiogenesis. J Clin Oncol 2005;23:1011–27.
22. Johrer K, Janke K, Krugmann J, Fiegl M, Greil R. Transendothelial migration of myeloma cells is increased by tumor necrosis factor (TNF)-α via TNF receptor 2 and autocrine up-regulation of CCL2. Clin Cancer Res 2004;10:1901–10.
23. Mazzucchelli L, Loetscher P, Kappeler A, et al. Monocyte chemoattractant protein-1 gene expression in prostatic hyperplasia and prostate adenocarcinoma. Am J Pathol 1996;149:501–9.
24. Loberg R, Day LL, Harwood J, et al. Monocyte chemoattractant protein-1 (CCL2) is a potent regulator of prostate cancer cell migration and proliferation *in vitro* and *in vivo*. Neoplasia 2006;8:578–86.
25. Kalikin LM, Schneider A, Thakur MA, et al. *In vivo* visualization of metastatic prostate cancer and quantitation of disease progression in immunocompromised mice. Cancer Biol Ther 2003;2:656–60.
26. Tannock IF, de Wit R, Berry WR, et al. Docetaxel plus prednisone or mitoxantrone plus prednisone for advanced prostate cancer. N Engl J Med 2004;351:1502–12.
27. Ben-Baruch A. The multifaceted roles of chemokines in malignancy. Cancer Metastasis Rev 2006;25:357–71.
28. Conti I, Rollins BJ. CCL2 (monocyte chemoattractant protein-1) and cancer. Semin Cancer Biol 2004;14: 149–54.
29. Condeelis J, Pollard JW. Macrophages: obligate partners for tumor cell migration, invasion, and metastasis. Cell 2006;124:263–6.
30. Peters W, Dupuis M, Charo IF. A mechanism for the impaired IFN-γ production in C-C chemokine receptor 2 (CCR2) knockout mice: role of CCR2 in linking the innate and adaptive immune responses. J Immunol 2000;165:7072–7.
31. Valente AJ, Graves DT, Vialle-Valentin E, Delgado R, Schwartz CJ. Purifications of a monocyte hemotactic factor secreted by nonhuman primate vascular cells in culture. Biochemistry 1988;27:4162.
32. Carr MW, Roth SJ, Luther E, Rose SS, Springer TA. Monocyte chemoattractant protein 1 acts as a T-lymphocyte chemoattractant. Proc Natl Acad Sci U S A 1994;91:3652.
33. Allavena P, Bianchi G, Zhou D, et al. Induction of natural killer cell migration by monocyte chemotactic protein-1, -2, and -3. Eur J Immunol 1994;24:3233.
34. Sallusto F, Schaerli P, Loetscher P, et al. Rapid and coordinated switch in chemokine receptor expression during dendritic cell maturation. Eur J Immunol 1998; 28:2760.
35. Youngs SJ, Ali SA, Taub SS, Rees RC. Chemokines induce migrational responses in human breast carcinoma cell lines. Int J Cancer 1997;71:257–66.
36. Bottazzi B, Colotta F, Sica A, Nobili N, Montovani A. A chemoattractant expressed in human sarcoma cells (tumor-derived chemotactic factor, TDCF) is identical to monocyte chemoattractant protein-1/monocyte chemotactic and activating factor (MCP1/MCAF). Int J Cancer 1990;45:795–7.
37. Mantovani A, Allavena P, Sica A. Tumour-associated macrophages as a prototypic type II polarized phagocyte population: role in tumor progression. Eur J Cancer 2004;40:1660–7.
38. Lu Y, Cai Z, Xiao G, et al. Monocyte chemotactic protein-1 mediates prostate cancer-induced bone resorption. Cancer Res 2007;67:3646–53.
39. Tucci M, Quatraro C, Frassanito MA, Silvestris F. Deregulated expression of monocyte chemoattractant protein-1 (MCP-1) in arterial hypertension: role in endothelial inflammation and atheromasia. J Hypertens 2006;24:1307–18.
40. Sarafi MN, Garcia-Zepeda EA, MacLean JA, Charo IF, Luster AD. Murine monocyte chemoattractant protein (MCP)-5: a novel CC chemokine that is a structural and functional homologue of human MCP-1. J Exp Med 1997;185:99–109.
41. Dewald O, Zymek P, Winkelmann K, et al. CCL2/monocyte chemoattractant protein-1 regulates inflammatory responses critical to healing myocardial infarcts. Circ Res 2005;96:881–9.